

Electrosprayed Microparticles with Loaded pDNA-Calcium Phosphate Nanoparticles to Promote the Regeneration of Mature Blood Vessels

Xueqin Guo · Tian Xia · Huan Wang · Fang Chen · Rong Cheng · Xiaoming Luo · Xiaohong Li

Received: 13 June 2013 / Accepted: 12 September 2013 / Published online: 25 September 2013
© Springer Science+Business Media New York 2013

ABSTRACT

Purpose The lack of control over microvasculature formation remains a key roadblock to the therapeutic vascularization and regeneration of functional tissues. In the current study, the integration of plasmid DNA (pDNA) condensation and electrospraying technologies was proposed to promote the regeneration of mature blood vessels through injectable or infusible administration of microparticles.

Methods Calcium phosphate (CP) nanoparticles with encapsulated plasmids encoding vascular endothelial growth factors (pVEGF) and basic fibroblast growth factor (pbFGF) were synthesized using reverse microemulsions. Electrosprayed microparticles with the loading of CP-pDNA nanoparticles were evaluated on both endothelial cells and smooth muscle cells and after subcutaneous infusion into animals.

Results CP-pDNA nanoparticles was obtained with an average size of around 110 nm and electrosprayed into microparticles, resulting in high loading efficiency and extended protection on pDNA from external DNase environment. The inoculation of poly(ethylene glycol) into microparticle matrices realized a gradual release for 4 weeks of CP-pDNA nanoparticles, leading to an incremental transfection efficiency and strong secretion of extracellular matrices. After subcutaneous infusion of microparticles with encapsulated both CP-pVEGF

and CP-pbFGF nanoparticles, significantly higher densities of blood vessels were achieved than those containing individual nanoparticles, and induced a rapid generation of mature blood vessels with few cytotoxicity and inflammation reactions.

Conclusions Electrosprayed microparticle with CP-pDNA nanoparticles encapsulated promoted the formation of vascular networks, providing clinical relevance for therapeutic vascularization and regeneration of functional tissues after injection to ischemic sites or entrapment into tissue engineering scaffolds.

KEY WORDS electrosprayed microparticle · extracellular matrix secretion · mature blood vessel · pDNA-loaded calcium phosphate nanoparticle · therapeutic vascularization

INTRODUCTION

Therapeutic angiogenesis plays a critical role in the treatment of ischemia, involving the formation of vascular networks *via* their sprouting from existing vessels. The development of blood vessels is also essential for the regeneration of complex tissues, since the diffusion of nutrients and metabolic products is sufficient only within a few millimeters. However, the lack of control over microvasculature formation remains a key roadblock to the therapeutic vascularization and regeneration of functional tissues (1). One approach to overcome this problem is to provide abundant angiogenic growth factors required to initiate the mobilization, adhesion, growth, and differentiation of progenitor cells. Among them vascular endothelial growth factor (VEGF) and basic fibroblast growth factor (bFGF) are the most important and widely studied signals (2). In clinical trials, the bolus injection of these growth factors into either the ischemic site or the systemic circulation suffers from a short half-life, no specific targeting, and unavailability for extended time periods to promote the initiation and mature of newly formed vessels (3). Therefore, it remains a great challenge

Electronic supplementary material The online version of this article (doi:10.1007/s11095-013-1209-y) contains supplementary material, which is available to authorized users.

X. Guo · H. Wang · F. Chen · X. Luo · X. Li (✉)
Key Laboratory of Advanced Technologies of Materials
Ministry of Education of China
School of Materials Science and Engineering
Southwest Jiaotong University
Chengdu 610031, People's Republic of China
e-mail: xhli@swjtu.edu.cn

T. Xia · R. Cheng
Department of Pathology, 452nd Hospital of People's Liberation Army
Chengdu 610021, People's Republic of China

to achieve delivery of growth factors specifically to target sites and maintain an effective level for a prolonged time period.

Attempts have been made to enhance a gradual and target delivery of growth factors. Formiga *et al.* loaded VEGF in poly(lactic-co-glycolic acid) microspheres to provide a sustained delivery of active protein for over one month, leading to a significant regeneration of blood vessels in ischemic tissues (4). But one major concern is the maintenance of structural integrity and biological activity of growth factors during processing and storage of the controlled release systems (5). The sustained delivery of plasmid DNA (pDNA) over a specific period provides a powerful alternative to produce angiogenic growth factors in transfect cells, and is generally advantageous in long-term effects and has lower costs compared to those of purified proteins. Although the local delivery of naked pDNA enhanced the angiogenesis and functional recovery of ischemic tissues (6), limitations with low gene transfer efficiency and rapid diffusion of pDNA from carriers motivated the use of pDNA complexes. The condensation of pDNA with cationic lipids and polymers has been investigated to achieve a significantly higher number of newly formed blood vessels than those with inoculation of free pDNA (7). Among them liposomal systems have been frequently applied *in vitro*, but require strictly controlled cell density and culture media, so it is difficult to apply this method *in vivo* (8). Poly(ethyleneimine) (PEI) is a widely investigated cationic polymer for nonviral gene delivery, but suffers from noticeable cytotoxicity and immune reactions thereby reducing their clinical relevance (9).

Calcium ions are capable of forming ionic complexes with the phosphates of pDNA and these complexes can be easily transported across the cell membrane *via* ion-channel mediated endocytosis (10). The concentrations of calcium and phosphate ions, respectively, decrease by 20,000-fold and increase by 40–70-fold between the extracellular and intracellular environments, leading to a selective dissolution of calcium phosphate nanoparticles once located inside cells (11). Another major advantage is that the solubility of calcium phosphate nanoparticles in the acidic endosome and lysosome is significantly higher than that at physiological pH (12), facilitating the intracellular delivery of pDNA. Attempts have been made to include pDNA-loaded calcium phosphate nanoparticles into tissue engineering scaffolds to induce sufficient protein expression during the tissue regeneration process. Curtin *et al.* developed a gene-activated matrix through incorporating calcium phosphate nanoparticles combined with pDNA into collagen-based scaffolds, indicating a high capacity for promoting bone formation when using low levels of plasmids (13). However, the continued aggregation and rapid

loss of the physiological stability in biological systems limit the application of calcium phosphate nanoparticles as gene delivery carriers (14). To address the stability issues, calcium phosphate-pDNA nanoparticles have been incorporated into liposomes or polymer matrices (11).

Various techniques can be used to produce microparticles with the most widely investigated methods being solvent evaporation from single or double emulsions and spray drying. However, there are some inevitable disadvantages associated with these methods, such as broad size distribution, low drug loading efficiency, and low yield of particles prepared by emulsification methods (15). Electro spraying is an emerging technique for the rapid and high throughput preparation of particles in nanometer to micrometer scale. Enayati *et al.* indicated that a strong electric field during electro spraying broke up a jet of polymer solution into a continuous stream of finely dispersed particles (16). Electro spraying techniques have potential advantages in cost and simplicity, and the direction of particles onto the collector under the electric field usually leads to a high production efficiency (17). Up to now the process parameters have been examined on the feature of electro sprayed particles, and the efficacy of drug-loaded particles has been primarily evaluated. Xie *et al.* fabricated paclitaxel-loaded particles with the size of over 10 μm by electro spraying, indicating a drug loading efficiency of around 80% and sustained release for more than 30 days (18).

This study was aimed to assess electro sprayed microparticles with loadings of pDNA-calcium phosphate (CP-pDNA) nanoparticles to allow a localized delivery for an efficient vascularization. As an injectable system, the administration of such microparticles to target tissues or into tissue engineering scaffolds can be easily achieved *via* established catheter-based or needle techniques. In the current study, CP nanoparticles with encapsulated pVEGF and bFGF-encoded plasmid (pbFGF) were synthesized using reverse microemulsions. Electro sprayed microparticles with loadings of the nanoparticles were prepared, and the pDNA release was modulated to adapt to the duration for the formation of mature blood vessels. Copolymer poly(ethylene glycol)-poly(DL-lactide) (PELA) was used as the microparticle matrix due to the compatibility between the matrix degradation and the formation of blood vessels (19). The cellular behaviors, including cell proliferation, transfection efficiency, and secretion of extracellular matrices (ECM) were evaluated *in vitro* on endothelial cells (ECs) and smooth muscle cells (SMCs). The extent of vascularization and vessel maturation were determined after subcutaneous infusion into animals *via* hematoxylin-eosin (HE) and immunohistochemical (IHC) staining.

MATERIALS AND METHODS

Materials

PELA ($M_w = 54.4$ kDa, $M_w/M_n = 1.23$) was prepared by bulk ring-opening polymerization of DL-lactide and poly(ethylene glycol) (PEG) using stannous chloride as initiator (20). The pVEGF, encoding fusion protein of VEGF/enhanced green fluorescent protein (eGFP), and pbFGF, encoding bFGF/eGFP fusion protein were purchased from FuluGen Co. (Guangzhou, China). The plasmids were transformed in *E. coli* DH5a, purified using Qiagen Giga kit (Hilden, Germany), and stored in Tris-EDTA buffer (10 mM Tris-HCl, 1 mM EDTA, pH 8.0) at 4°C. All the electrophoresis reagents, PEG ($M_w = 2, 4,$ and 6 kDa), bovine serum albumin (BSA), 4',6-diamidino-2-phenylindole (DAPI), and bisbenzimidazole (Hoechst 33258) were procured from Sigma (St. Louis, MO). Protein molecular weight marker and RIPA lysis buffer were from Beyotime Institute of Biotechnology (Shanghai, China). Rabbit anti-human antibodies of collagen I, collagen IV, laminin, α -smooth muscle actin (α -SMA) and β -actin, rabbit anti-rat antibodies of CD31, collagen IV and α -SMA, goat anti-rabbit IgG-horseradish peroxidase (HRP), goat anti-rabbit IgG-fluorescein isothiocyanate (FITC) and 3,3'-diaminobenzidine (DAB) developer were purchased from Boster Bio-engineering Co., Ltd. (Wuhan, China). All other chemicals were of analytical grade and received from Changzheng Regents Company (Chengdu, China) unless otherwise indicated.

Preparation of CP-pDNA Nanoparticles

The preparation of CP-pDNA nanoparticles was synthesized using reverse microemulsions as described previously with some modifications (21). Briefly, microemulsions were formed in cyclohexane as the oil phase containing 10% (v/v) OP-10. Aqueous phase of 0.5 ml containing 20 mg $\text{Ca}(\text{NO}_3)_2$ and 250 μg pDNA was emulsified into 15 ml oil phase by continuous stirring for 1 h to form microemulsion A. Similarly, microemulsion B was formed by emulsifying 0.5 ml of water containing 10 mg $(\text{NH}_4)_2\text{HPO}_4$ and 250 μg pDNA into 15 ml oil phase. Microemulsion B was slowly added to microemulsion A at a rate of 5 ml/h with continuous stirring, and the mixture was adjusted to pH 9.0 by 1 M ammonia. The resulting solution was stirred for another 1 h, followed by centrifugation to collect nanoparticles. The nanoparticles were washed with ethanol three times, and lyophilized to obtain CP-pDNA nanoparticles. Empty CP nanoparticles were prepared without pDNA addition in above microemulsions.

Electrospraying of Microparticles with CP-pDNA Nanoparticles Loaded

PELA microparticles with CP-pDNA nanoparticles loaded (CP-pDNA/PELA) were prepared by electrospraying as

described previously with some modifications (22), and PEG was blended with PELA before electrospraying to modulate the release of CP-pDNA nanoparticles from microparticle matrices. Briefly, CP-pDNA nanoparticles were dispersed in double distilled water by sonication, which was emulsified into dimethylformide containing 450 mg of PELA and 50 mg of PEG. The resulting dispersion was placed in a 2-ml syringe and was continuously pushed by a syringe pump (Zhejiang University Medical Instrument, Hangzhou, China) at a flow rate of 4 ml/h. A high-voltage power supply (Tianjing High Voltage Power Supply Co., Tianjing, China) was used to generate a 20 kV potential difference. A spraying distance of 10 cm was set between the syringe nozzle with the size of 0.55 mm and the grounded copper foil, which was immersed in a water bath of around 5 mm in depth. The microparticles were collected by centrifugation, lyophilized overnight to remove any solvent and water residues, and stored at 4°C. Electrosprayed microparticles with the encapsulation of CP-pVEGF, CP-pbFGF nanoparticles and both of them were prepared as Pv, Pb and Pv-b, respectively. PEG with M_w of 2, 4 and 6 kDa was blended with PELA to obtain P2, P4 and P6 microparticles, respectively. Empty microparticles without pDNA inoculation were also prepared as P₀. In order to visualize the distribution of CP-pDNA nanoparticles in electrosprayed microparticles, pDNA was labeled with DAPI, which was electrosprayed into CP-dapi-pDNA/PELA microparticles.

Characterization of CP-pDNA Nanoparticles and Electrosprayed Microparticles

The morphologies of CP-pDNA nanoparticles were examined by an atomic force microscope (AFM, CSPM5000, Beijing, China) after the sample-loaded silicon wafer was air-dried at room temperature. The aqueous suspensions of electrosprayed microparticle were dropped on a metal stub, sputter-coated with gold, and observed by a scanning electron microscope (SEM, FEI Quanta200, The Netherlands) equipped with a field-emission gun and Robinson detector. The size and Zeta potential of CP-pDNA nanoparticles were measured by a Nano-ZS laser particle analyzer (Zetasizer Nano ZS90, Malvern Co. UK), while the size of electrosprayed microparticles was examined by a laser diffraction particle size analyzer (Horiba LA920, Japan). The encapsulation of CP-dapi-DNA nanoparticles in electrosprayed microparticles was observed under a confocal laser scanning microscope (CLSM, Leica TCS SP2, Germany), with an excitation wavelength of 364 nm and an emission wavelength of 454 nm.

To determine the pDNA encapsulation efficiency, CP-pDNA nanoparticles were extracted three times with phosphate buffer solution (PBS) containing 10 mg/ml heparin, while electrosprayed particles were dissolved in dichloromethane,

followed by extraction three times with PBS containing 10 mg/ml of heparin. The extract was mixed with Hoechst 33258 and the fluorescence intensity was measured by a fluorospectrophotometer (Hitachi F-7000, Japan) at an excitation wavelength of 350 nm and an emission wavelength of 450 nm (23). The encapsulation efficiency indicated the amount of pDNA encapsulated compared with the total amount used for the particle preparation. The protective effect of CP nanoparticles and electrosprayed microparticles on the structural integrity of pDNA was determined by DNase I digestion as described previously (23), using free pDNA and free pDNA-adsorbed empty nanoparticles (CP + pDNA) as control. After incubation for up to 48 h, pDNA was extracted as above, and electrophoresized in 1% agarose gel, which was viewed by a gel documentation system (Bio-RAD, Hercules, CA) to determine the structural integrity of pDNA.

In Vitro pDNA Release from Electrosprayed Microparticles

Electrosprayed microparticles were sterilized by electron-beam irradiation using linear accelerator (Precise™, Elekta, Crawley, UK) with a total dose of 80 cGy. The particles were immersed in 5.0 ml of PBS, which was kept in a thermostated shaking water bath that was maintained at 37°C and 100 cycles/min. At predetermined time intervals, 0.2 ml of the release buffer was removed for analysis and an equal volume of fresh buffer was added back to the release media. The release buffer retrieved was electrophoresized in 1% agarose gels to determine the presence of CP-pDNA nanoparticle. The retrieved buffer was also incubated in 10 mg/ml heparin solution, and the pDNA amount was determined with Hoechst 33258 as described above.

Cell Viability and Transfection after Incubation with Electrosprayed Microparticles

Human umbilical vein ECs and human aortic SMCs from American Type Culture Collection (Rockville, MD) were used to examine the cell viability, gene transfection efficiency, and ECM secretion. ECs and SMCs were maintained in Dulbecco's modified Eagle's medium (DMEM, Gibco BRL, Rockville, MD) supplemented with 10% heat inactivated fetal bovine serum (FBS, Gibco BRL, Grand Island, NY). EC or SMC suspensions with a cell density of 5×10^4 cells/ml were seeded in 24-well tissue culture plates (TCP). After 24 h incubation to allow cell attachment, sterilized electrosprayed microparticles Pv, Pb and Pv + b were added in each well. After incubation for 48 h, the cell viability was assayed with cell counting kit (CCK-8, Dojindo Molecular Technologies, Inc., Kumamoto, Japan) as described previously (23). Another batch of cells were used for the cell transfection assay after incubation for 48 h. Cells were also treated with empty

microparticles plus CP-pVEGF, CP-pbFGF nanoparticles and both of them, which were named as $P_0 + v$, $P_0 + b$ and $P_0 + v-b$ particle mixtures, respectively. After removal of culture media, cells were fixed with 4% paraformaldehyde, and GFP expression was observed by a fluorescence microscope (Leica DMR HCS, Germany). The cells were incubated with RIPA lysis buffer, and the level of pDNA transfection was determined from the relative light unit (RLU) of the cell lysate, normalized to the total protein as described previously (23).

ECM Secretion after Incubation with Electrosprayed Microparticles

The production of collagen IV and laminin by ECs, and that of collagen I and α -SMA by SMCs were determined by immunofluorescent staining. Briefly, cells cultured on glass slides for 48 h as above were washed with PBS, fixed with 4% paraformaldehyde and permeabilized with 0.1% Triton X-100 solution in PBS. The glass slides were incubated with rabbit anti-human antibodies for 2 h at 37°C. After incubation with secondary FITC-conjugated antibody at room temperature for 1 h, the slides were mounted and observed by CLSM with the excitation and transmission wavelengths of 488 and 535 nm, respectively. Western blot was used to determine collagen IV secretion by ECs, and α -SMA secretion by SMCs. Briefly, cells were cultured for 48 h, and lysed as above. The lysate was electrophoresized on 10% SDS-PAGE gel at 100 V, followed by transfer to a PVDF membrane (Millipore Corp., Bedford, MA). The membrane was washed and incubated with rabbit anti-human antibodies for 1 h at room temperature and kept at 4°C overnight. The membrane was then washed and incubated with secondary HRP-conjugated antibody for 1 h, and the antigen-antibody complexes were visualized by DAB developer. Expression of β -actin was used as protein loading control.

Subcutaneous Infusion of Electrosprayed Microparticles

The angiogenesis promotion was evaluated after subcutaneous infusion of electrosprayed microparticles, and all animal procedures were approved by the University Animal Care and Use Committee. Male Sprague-Dawley rats, from Sichuan Dashuo Biotech Inc. (Chengdu, China), weighing 110 to 140 g, were denuded on the back with 8% Na_2S aqueous solution. The rats were anesthetized by intraperitoneal injection of pentobarbital sodium at a dosage of 30 mg/kg. Electrosprayed microparticles were dispersed into alginate solution, which was subcutaneously infused along with CaCl_2 solution using a dual-lumen catheter to form a gel (24). pDNA-loaded electrosprayed microparticles Pv, Pb and Pv + b were tested, using empty microparticles P_0 , and particle mixtures $P_0 + v$, $P_0 + b$ and $P_0 + v-b$ as control. Two subcutaneous

infusions were made on each side of the back, and four samples were tested for each group.

Characterization of Blood Vessel Formation

After 1, 2 and 4 weeks of administration, subcutaneous tissues around the infusion site were explanted. One part of the tissues retrieved from each group were frozen and sectioned for HE staining to evaluate the inflammatory reaction, tissue infiltration and blood vessel formation. Another part of the tissues were paraffin-embedded and sectioned for IHC staining of CD31, collagen IV and α -SMA (19). The stained sections were observed with a light microscope (Nikon Eclipse E400, Japan). A minimum of 10 individual images were randomly chosen from IHC stained sections of each sample to count the positively stained vessels with morphological circumference (19). The blood vessel density was normalized to the tissue area (number of vessels/mm²).

Statistics Analysis

The values were expressed as means \pm standard deviation (SD). Whenever appropriate, two-tailed Student's *t*-test was used to discern the statistical difference between groups. A probability value (*p*) of less than 0.05 was considered to be statistically significant.

RESULTS AND DISCUSSION

Characterization of CP-pDNA Nanoparticles

Figure 1a shows the AFM image of CP-pDNA nanoparticles, possessing uniform spherical shape and smooth surface without serious aggregation. The nanoparticles had a size of 111 ± 14 nm, Zeta potential of -10.9 ± 0.7 mV and pDNA encapsulation efficiency of $89.9 \pm 2.4\%$. Calcium phosphate exhibits a high binding affinity for pDNA most likely due to the interactions between calcium ions and the negatively charged phosphate groups of pDNA, and thus may enhance the stabilities of certain pDNA structures (25). It is known that the physicochemical properties of calcium phosphate, such as the solubility and lattice structures, are highly dependent on their components (26). In the current study, nanoparticles with varying Ca/P ratios were generated to determine the influence of Ca/P stoichiometry on the particle size, cytotoxicity and gene transfection efficiency. The particular preparation methods and characterization results are included in the [Supplementary Materials](#). Through controlling the Ca/P feeding ratios (1/1, 4/3, and 5/3) and pH values of the reaction media (from 6.0 to 9.0), dicalcium phosphate dihydrate (DCPD), octacalcium phosphate (OCP) and hydroxyapatite (HA) were formed in CP-pDNA nanoparticles (Fig. S1).

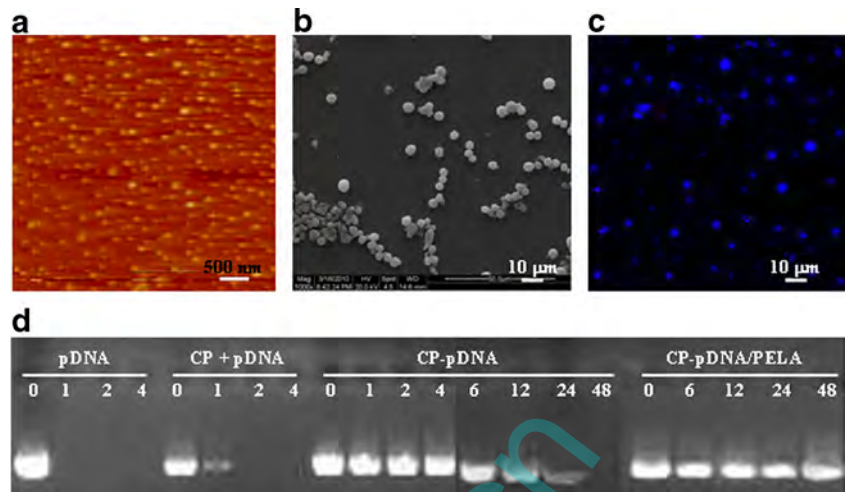
The cytotoxicity and transfection efficiency of CP-pDNA nanoparticles with different compositions were determined on ECs and SMCs compared with pDNA polyplexes with PEI. As shown in Table S2, significantly lower cell viability and higher transfection efficiency were found for PEI-pDNA polyplexes than those of CP-pDNA nanoparticles ($p < 0.05$). The total protein was significantly lower because of the cytotoxicity of PEI-pDNA polyplexes, resulting in the higher transfection efficiency represented by relative fluorescence intensity (RLU/mg protein) compared with CP-pDNA nanoparticles. As shown in Table S2, HA-pDNA nanoparticles revealed a slightly lower cytotoxicity than other CP-pDNA nanoparticles, which may be attributed to the lower water solubility of HA under neutral pH (27). But the selective dissolution of pDNA from carriers once located inside cells determined the transfection efficiency, and the endocytosed calcium phosphate nanoparticles were expected to deassemble in the endosomes and release the bound DNA into the cytoplasm. Compared with those of OCP and DCPD, the water solubility of HA indicated a higher sensitivity to the acidic environments (27), resulting in higher transfection efficiencies on both ECs and SMCs. Therefore, HA-pDNA nanoparticles were used in the following study.

Characterization of Electrospayed Microparticles

Figure 1b shows the SEM morphology of electrospayed microparticles with a diameter of 3.5 ± 0.5 μ m. Figure 1c showed the CLSM image of CP-dapi-DNA/PELA microparticles, and the blue fluorescence indicated that CP-dapi-DNA nanoparticles had been electrospayed into microparticles. The pDNA loading efficiency into electrospayed microparticles was $87.2 \pm 5.6\%$. The electrospayed liquid droplets were rapidly solidified into particles during flying to the collector, resulting in a high loading efficiency (28).

The structural integrity of pDNA after entrapped in CP nanoparticles and electrospayed microparticles was determined after exposure to DNAase I. As shown in Fig. 1d, free pDNA was completely digested by DNase within 1 h of incubation. The level of protection offered to pDNA absorbed on empty CP nanoparticles was also extremely low and pDNA was prone to nearly total degradation within 2 h of incubation. CP-pDNA nanoparticles protected pDNA from digestion by equal mass of DNase I for up to 6 h, while pDNA lost the structural integrity after that. It should be noted that pDNA entrapped within electrospayed microparticles remained intact after incubation with DNase I for 48 h. These results indicated that electrospayed microparticles and CP nanoparticles could protect pDNA encapsulated from nuclease digestion, and

Fig. 1 (a) AFM image of CP-pVEGF nanoparticles. (b) SEM and (c) CLSM images of electrosprayed microparticles Pv-b. (d) Agarose gel electrophoresis analysis of pVEGF extracted from CP-pVEGF nanoparticles and CP-pVEGF/PELA microparticles after incubation with DNase I for up to 48 h, using free pVEGF, free pVEGF-absorbed empty CP nanoparticles (CP + pVEGF) as control.



the polymer matrices enabled a significantly higher protection from external DNase environment.

In Vitro pDNA Release from Electrosprayed Microparticles

Figure 2a summarizes the percent release of pDNA from electrosprayed microparticles, indicating an apparent initial burst release during 24 h, followed by a sustained release over an extended time period. After an initial release of around 18%, there was around 30% of gradual release from electrosprayed microparticles without PEG inoculation during 30 days of incubation. Owing to the size of around 110 nm and the interactions with matrix polymers, CP-pDNA nanoparticles did not diffuse appreciably into the release media until the matrix polymers had been significantly degraded. In the current study, 10% of PEG with M_w of 2, 4 and 6 kDa was blended into microparticle matrices to modulate the pDNA release. The PEG inoculation was supposed to accelerate the matrix hydration, create microscopic holes after PEG dissolution, and increase the contact area of matrix polymers with media (23), promoting the release of CP-pDNA nanoparticles from microparticles. As shown in Fig. 2a, the sustained release rate of pDNA from microparticles was dependent on the M_w of PEG. The duration of pDNA release could be modulated within 13, 23 and over 30 days from microparticles containing PEG of 6, 4 and 2 kDa, respectively. This can be attributed to the fact that the longer the molecular chains of PEG were, the larger channels and cavities were there after dissolution, which could promote medium exchange so as to release faster of CP-pDNA nanoparticles entrapped. Figure 2b shows the electrophoresis images of pDNA released at different time intervals. Compared with free pDNA incubated in PBS, clear fluorescence was observed in sample holes, indicating

that the pDNA released was integrated with CP nanoparticles, and only few of them was free pDNA.

Cell Viability and Transfection Efficiency of Electrosprayed Microparticles

Figure 3 shows the cell viability after incubation with electrosprayed microparticles of different doses from 12.5 to

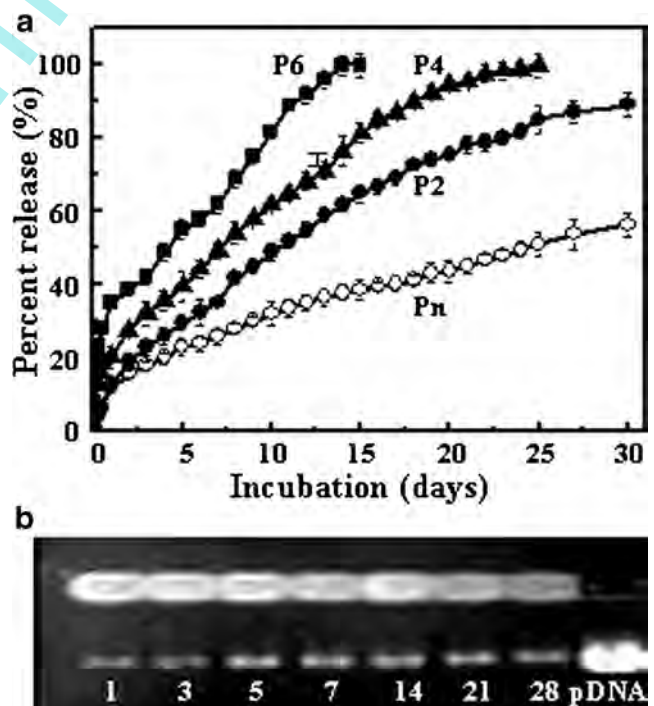


Fig. 2 (a) Percent release of pVEGF from electrosprayed CP-pDNA/PELA microparticles containing 10% PEG of 2 (P2), 4 (P4), and 6 kDa (P6), compared with those without PEG inoculation (Pn) after incubation in PBS, pH 7.4 at 37°C ($n = 3$). (b) Agarose gel electrophoresis analysis of pVEGF released from microparticles at different time points with free pVEGF incubated in PBS as control.

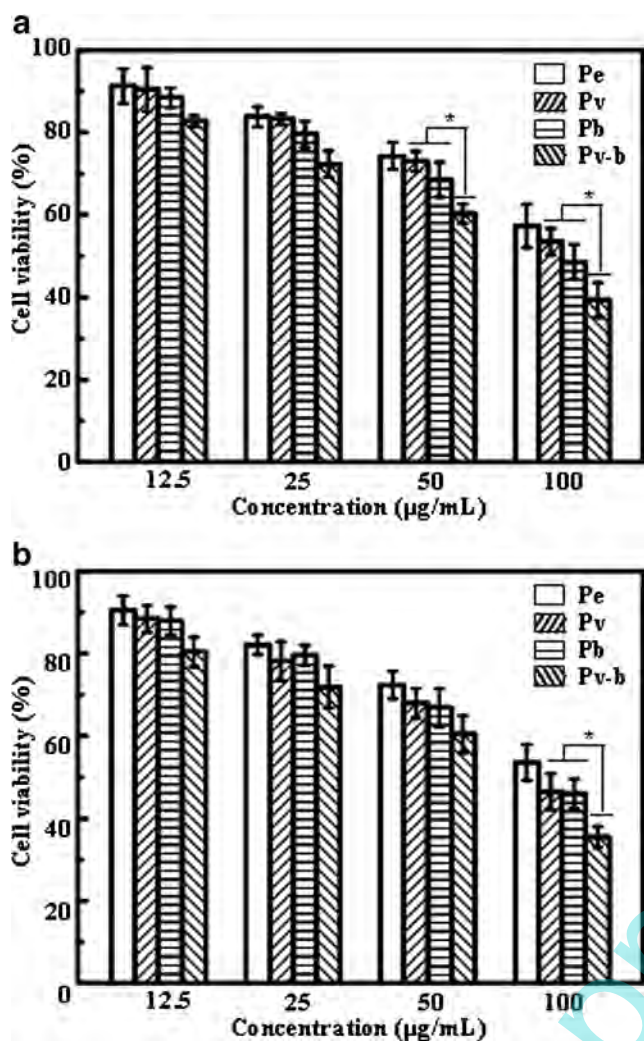


Fig. 3 The viability of (a) ECs and (b) SMCs after incubation with micro-particles containing empty CP nanoparticles (Pe), Pv, Pb and Pv-b micro-particles at different doses for 48 h ($n = 6$). *: $p < 0.05$.

100 µg/ml. There was no significant difference in the viabilities between ECs and SMCs at each micro-particle concentration, and both of them decreased with the increase in the micro-particle concentrations. As shown in Fig. 3, the cell viability was around 80% after incubation with micro-particles of 25.0 µg/ml, which was used in the following tests on the cell transfection efficiency. There was no significant difference among empty micro-particles, micro-particles with encapsulation of pVEGF or pbFGF ($p > 0.05$). But micro-particles with the inoculation of both pVEGF and pbFGF indicated a slightly lower cell viability than those including only one plasmid.

Cells transfected with pVEGF and pbFGF should express fusion proteins of VEGF/eGFP and bFGF/eGFP, respectively. The transfection efficiency was determined on ECs and SMCs after being cultured with Pv, Pb and Pv-b, compared with $P_0 + v$, $P_0 + b$ and $P_0 + v-b$ particle mixtures. As shown in Fig. 4, compared with the particle mixtures, CP-pDNA-

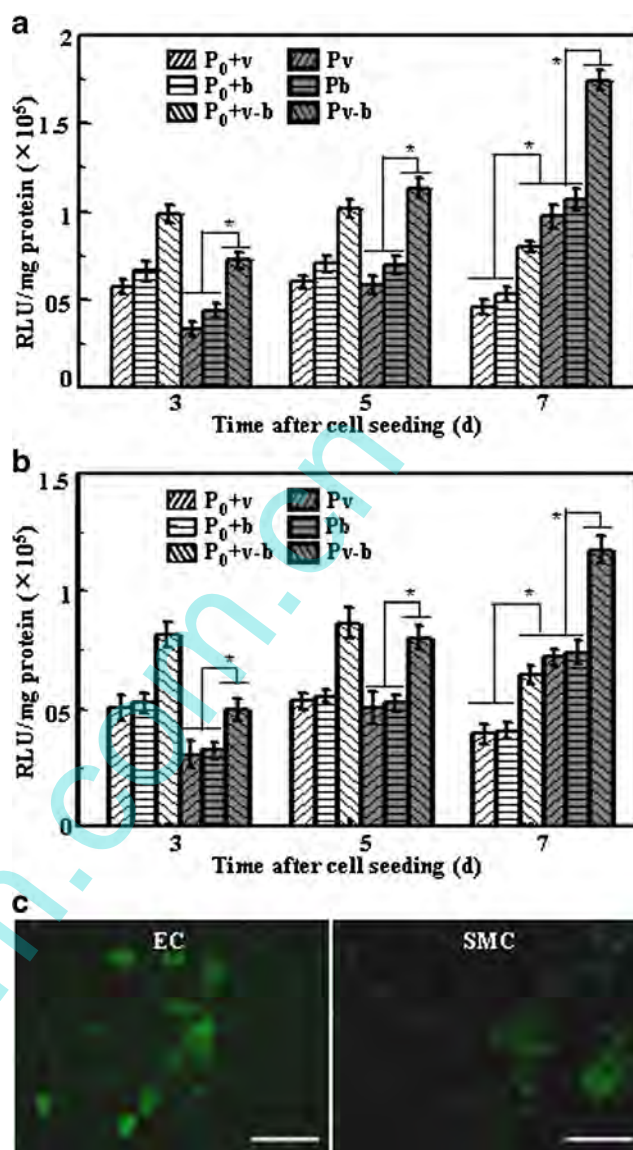


Fig. 4 Transfection efficiency of (a) ECs and (b) SMCs after incubation with Pv, Pb and Pv-b micro-particles for different time periods, compared with $P_0 + v$, $P_0 + b$ and $P_0 + v-b$ particle mixtures ($n = 6$). *: $p < 0.05$. (c) Fluorescence microscope images of ECs and SMCs after incubation with Pv-b for 7 days. Bars represent 10 µm.

loaded micro-particles indicated a significantly lower transfection efficiency after 3 days of incubation ($p < 0.05$), comparable efficiency after 5 days ($p > 0.05$), but significantly higher transfection after 7 days ($p < 0.05$). One possible reason was the disintegration of CP-pDNA nanoparticles in the cell culture media with the extension of time. But CP-pDNA nanoparticles released from electro-sprayed micro-particles should keep an intact structure and maintain the transfection capabilities. As indicated above, the gradual release of CP-pDNA nanoparticles led to a sustained expression of VEGF and bFGF to stimulate cell growth, resulting in persistent and incremental transfection efficiencies for Pv, Pb and Pv-b. In addition, the transfection of CP-pDNA nanoparticles was not

resulted in the incorporation of pDNA into the host genome, so the transient transfection should be diluted with the increased viability of cells. As shown in Fig. 4, a decrease in the transfection efficiency was detected on cells after incubation with particle mixtures for 7 days.

As shown in Fig. 4, there was a similar phenomenon at each time points, that is to say, the transfection efficiencies of groups treated with both pVEGF and pbFGF were higher, regardless of $P_0 + v-b$ and $Pv-b$, than that of groups treated with individual pDNA. Compared with Pv microparticles, $Pv-b$ microparticles indicated an increase of 50–70% in the GFP expression, at $(1.74 \pm 0.05) \times 10^5$ and $(1.17 \pm 0.06) \times 10^5$ RLU/mg protein after 7 days of incubation with ECs and SMCs, respectively. The differences in the transfection efficiency should be resulted from the expression of bFGF/eGFP and pVEGF/eGFP for $Pv-b$ microparticles. Figure 4c shows the transfect cells of $Pv-b$ microparticles after 7 days of incubation, both emitting green fluorescence, and a slightly stronger GFP expression was observed on ECs than that of SMCs.

ECM Secretion of ECs and SMCs

The basal lamina of microvessels is composed of collagen, proteoglycans and glycoproteins, and the deposition of these ECM macromolecules indicated an important role of ECs and substantial functions in the vascular formation (29). SMCs play an important role in the maintenance of arterial integrity and functions. The growth of SMCs is characterized by expression of cytoskeletal and contractile proteins such as α -SMA, myosin, collagen I, and elastin (30). In the present study, the immunofluorescent staining of collagen IV and laminin was determined on ECs and that of collagen I and α -SMA on SMCs after 7 days of culture with Pv , Pb and $Pv-b$, compared with $P_0 + v$, $P_0 + b$ and $P_0 + v-b$ particle mixtures. Figure 5a shows typical images of the immunofluorescent staining. A stronger expression of extracellular proteins was observed for $Pv-b$ microparticles than that of $P_0 + v-b$, and similar results were obtained for both ECs and SMCs.

The collagen IV expression by ECs and α -SMA expression by SMCs were evaluated by Western blotting after 7 days of incubation, and Fig. 5b summarizes the results. As seen from the band densities, the amount of collagen IV and α -SMA extracted from cells treated with $Pv-b$ microparticles was significantly higher than those from other microparticles, which should be ascribed to the simultaneous expression of VEGF and bFGF. The ECM secretions of CP-pDNA nanoparticles-loaded microparticles were higher than those of corresponding particle mixtures, reflecting results similar to the transfection tests (Fig. 4). In addition, compared with the promotion effect of bFGF on both ECs and SMCs (31), VEGF was beneficial to the proliferation of ECs, but could not promote or inhibit SMCs to grow nearly (32). As shown in Fig. 5b, the band intensity of collagen IV for Pv -treated ECs

was higher than that of Pb , while there was no apparent difference for SMCs.

Histological Staining of Tissues Grown after Subcutaneous Infusion

After subcutaneous administration the microparticles-loaded alginate gel was swollen and broken along with cell ingrowth. Histological staining of the tissues retrieved to investigate the inflammatory reaction and the formation of blood vessels. In our previous study, the implantation of electrospun fibers with loading of PEI-pDNA polyplexes led to strong inflammation both between fibrous layers and at the interface of fibrous mats with penetrated tissues, and necrotic tissues were observed followed by scar formation (19). As shown in Fig. 6a, macrophages were indicated with tissues penetration into the implants at week 1. There was no significant difference in the amount of inflammatory cells after administration of P_0 , $P_0 + v-b$ and $Pv-b$ microparticles, indicating that the presence of CP-pDNA nanoparticles resulted in no significant inflammatory reaction. HE staining of tissues retrieved after 4 weeks of administration indicated no inflammatory cell remaining, while blood vessels were formed after cell infiltration into implants and arrangement into a circular structure. As shown in Fig. 6b, the vascular density of $Pv-b$ was significantly higher than those of $P_0 + v-b$ and P_0 , indicating that the sustained release of CP-pDNA nanoparticles and sustained express of growth factors promoted the angiogenesis in a long time. As shown in the inset of Fig. 6b, red blood cells were found in the vessel-like structures, indicating that the newly formed vessels were integrated with native vasculature.

IHC Staining of Collagen IV and α -SMA

Mature blood vessels are characterized by a layer of ECs surrounded by SMCs and pericytes in the walls. CD31 was used primarily to demonstrate the presence of ECs, and the deposition of collagen IV indicated a similar distribution of ECs (33), while α -SMA was used to study the maturation levels of newly formed blood vessels (34). Figure 7 shows IHC staining results of CD31 and collagen IV, indicating a circular morphology in all the tissue sections. The total number of blood vessels was manually counted from the circles with collagen IV-positive staining (35). As shown in Fig. 7, there was no significant difference in the vessel densities of all the test groups after 1 week of administration ($p > 0.05$). A slight increase in the vessel densities was observed at week 2 after administration of $P_0 + v$, $P_0 + b$ and $P_0 + v-b$ particle mixtures, but remained no significant change at week 4 ($p > 0.05$). The positively stained vessels gradually increased after administration of CP-pDNA-loaded microparticles, at 210 ± 17 , 182 ± 16 and 248 ± 18 vessels/mm² for Pv , Pb and $Pv-b$ microparticles at week 4, respectively. The treatment with Pv -

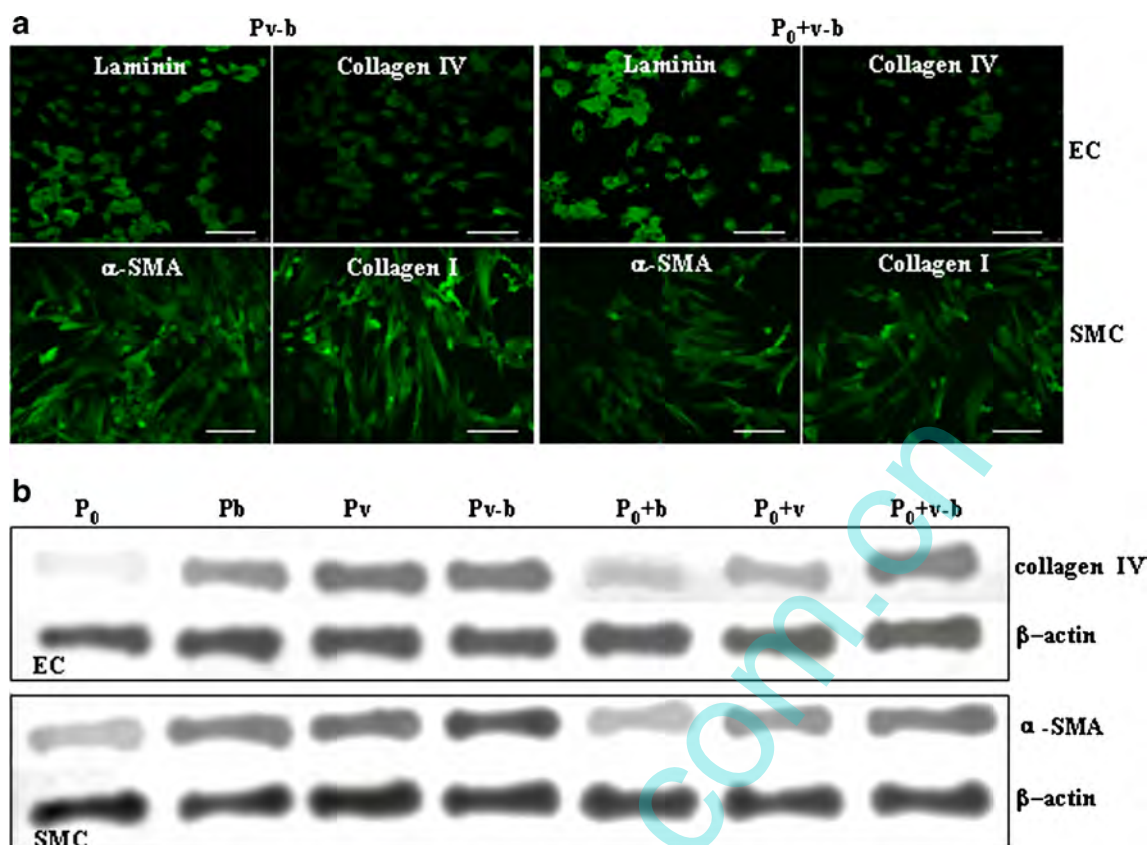


Fig. 5 (a) Immunofluorescent staining images of collagen IV and laminin expressions by ECs, and collagen I and α -SMA expressions by SMCs after incubation for 7 days with Pv-b microparticles and P₀ + v-b particle mixtures. Bars represent 50 μ m. (b) Western blotting assay of collagen IV expressions by ECs and α -SMA expressions by SMCs after incubation for 7 days with Pv, Pb and Pv-b microparticles, P₀ + v, P₀ + b and P₀ + v-b particle mixtures, and P₀ empty microparticles. Total proteins were prepared from cell lysate, and β -actin was used as protein loading control.

b microparticles indicated significantly higher vessel densities than other groups ($p < 0.05$).

Figure 8 shows IHC staining images for α -SMA expression of tissue explants, indicating the existence of α -SMA-secreting

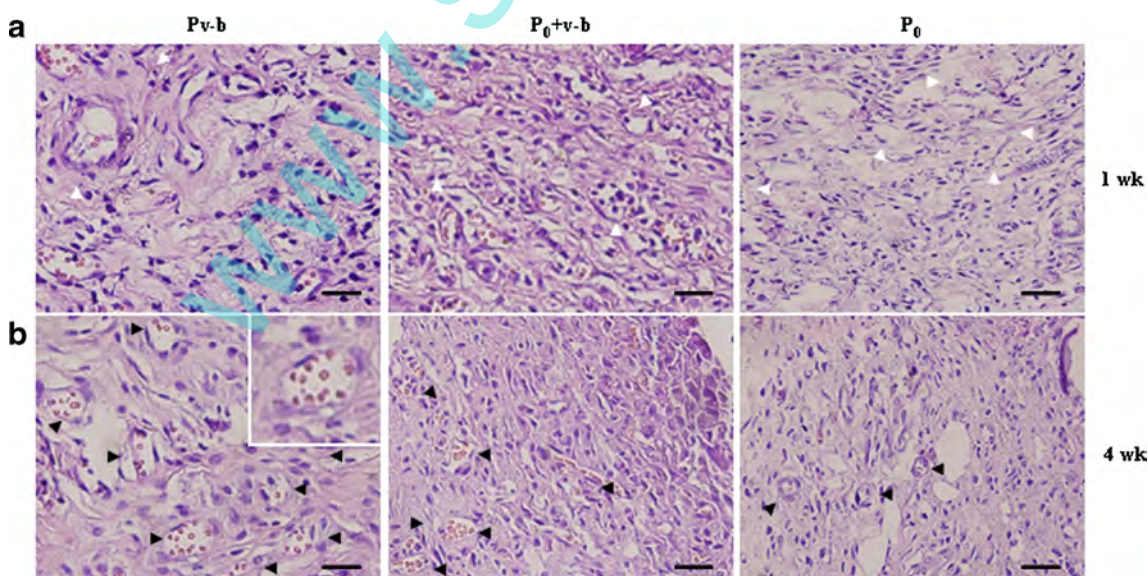


Fig. 6 Inflammatory reaction and blood vessel formation observed by HE staining on tissue sections at week 1 (a) and 4 (b) after administration of Pv-b microparticles, P₀ + v-b particle mixtures and P₀ empty microparticles. White arrow heads indicate inflammatory cells, and black ones blood vessels. Inset indicates a vessel with filled red blood cells. Bars represent 20 μ m.

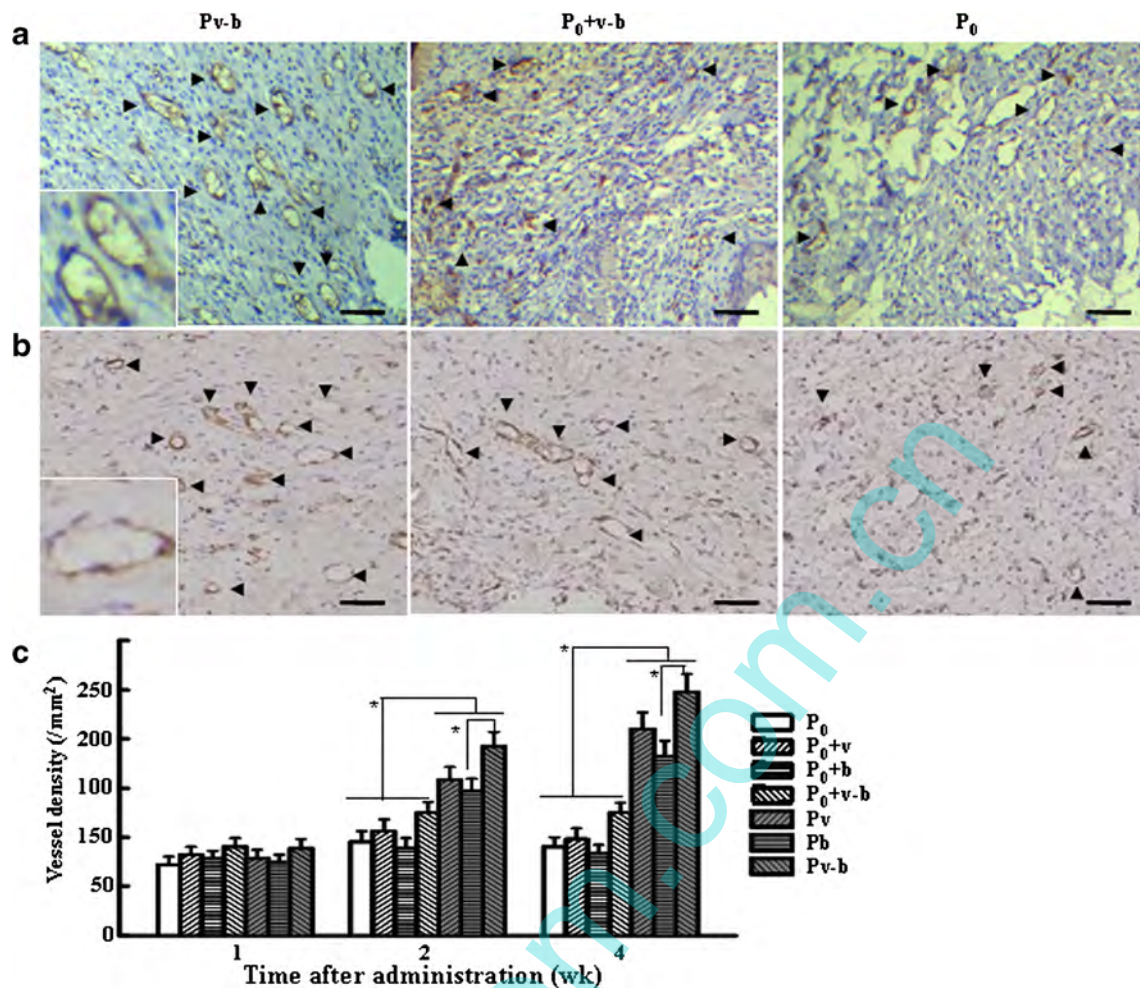


Fig. 7 IHC staining images for (a) CD31 and (b) collagen IV expressions of tissue explants treated with Pv-b microparticles, P₀ + v-b particle mixtures and P₀ empty microparticles for 4 weeks. Arrow heads indicate collagen IV-positive vessels with morphological circumference, and inserts show high magnification images. Bars represent 200 μ m. **c** Quantitative counts of collagen IV-positive vessels and normalized to tissue area (# vessels/mm²) after 1, 2 and 4 weeks of administration of Pv, Pb and Pv-b microparticles, P₀ + v, P₀ + b and P₀ + v-b particle mixtures, and P₀ empty microparticles. *: $p < 0.05$.

cells, such as SMCs and pericytes in the walls of newly formed blood vessels. α -SMA positive staining was used as a marker for mature blood vessels (35), and the quantitative results of mature vessel densities after 1, 2 and 4 weeks of administration are shown in Fig. 8b. The densities of mature blood vessels were around 50 vessels/mm² for all the test groups after 1 week of administration. There was no significant difference in the α -SMA positive staining at week 2 and 4 compared with that at week 1 after administration of P₀, P₀ + v, P₀ + b and P₀ + v-b ($p > 0.05$). However, the microvessel density indicated a significant increase after encapsulation of CP-pDNA nanoparticles into microparticles. At week 4, the densities of mature vessels were 168 ± 13 , 152 ± 13 and 233 ± 17 vessels/mm² for Pv, Pb and Pv-b microparticles, respectively, which were significantly higher than those of other groups ($p < 0.05$). As shown in Fig. 8b, Pv-b microparticles with inoculation of both pbFGF and pVEGF led to significantly higher densities

of mature blood vessels than Pv and Pb after 2 and 4 weeks of administration ($p < 0.05$).

Blood Vessel Regeneration after Treatment with CP-pDNA-Loaded Microparticles

The development of microvessel networks is playing significant roles in the establishment of complex tissues and the treatment of ischemic disease, which require capillary networks to provide sufficient supply of nutrients and removal of waste products. Formiga *et al.* loaded VEGF into microparticles for revascularization, indicating capillaries mostly and irregularly shaped blood vessel in the regenerated tissue. It can be ascribed to the fact that growth factors would easily be disintegrated by enzymes in the body, and can not remain uninterrupted and steady activities (4). The integration of pDNA condensation techniques in tissue engineering

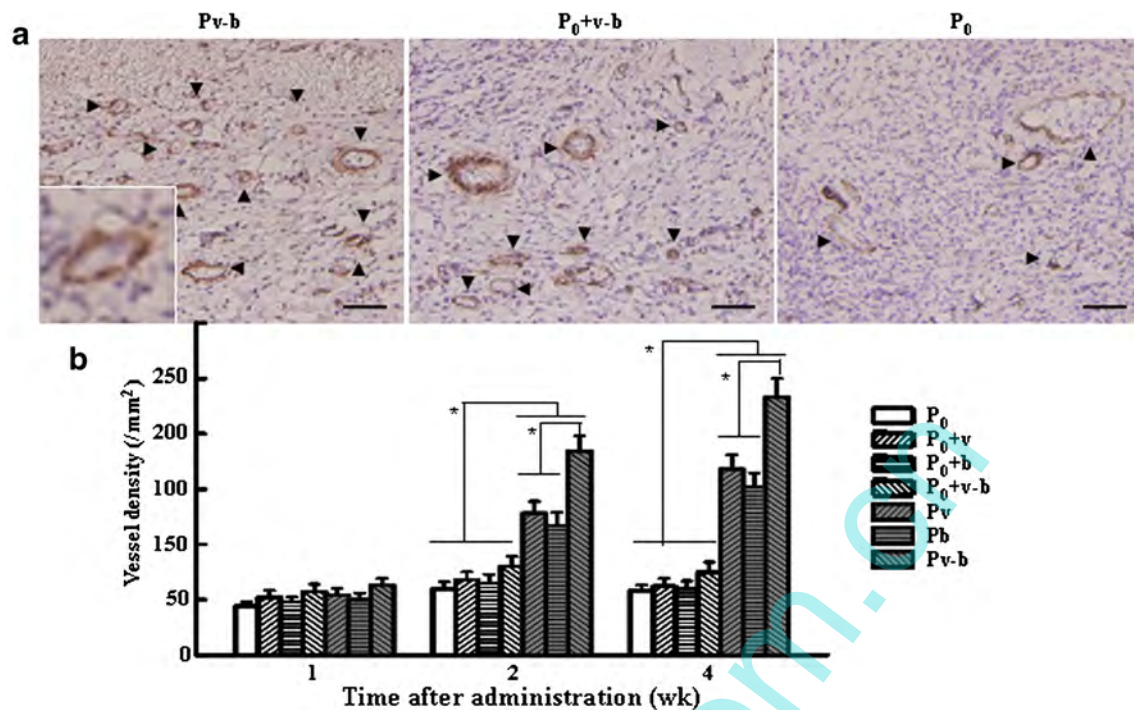


Fig. 8 (a) IHC staining images for α -SMA expressions of tissue explants treated with *Pv-b* microparticles, $P_0 + v$ -b particle mixtures and P_0 empty microparticles for 4 weeks. Arrow heads indicate α -SMA-positive vessels with morphological circumference, and insert shows a high magnification image. Bars represent 200 μ m. (b) Quantitative counts of α -SMA-positive vessels and normalized to tissue area (# vessels/mm²) after 1, 2 and 4 weeks of administration of *Pv*, *Pb* and *Pv-b* microparticles, $P_0 + v$, $P_0 + b$ and $P_0 + v$ -b particle mixtures, and P_0 empty microparticles. *: $p < 0.05$.

scaffolds was supposed to realize a localized transfection of cells and provide sufficient protein to enhance new tissue formation. In addition, the gradual and local release of pDNA could reduce angiogenic disorders, such as uncontrolled angiogenesis and angiogenesis in nontarget sites (36). PEI is a widely utilized cationic polymer for pDNA condensation, and Ye *et al.* investigated the local delivery of PEI-pVEGF polyplexes for myocardial repair during acute myocardial infarction. The formation of new blood vessels was determined after 2 weeks with improved cardiac function, but significant cytotoxicity was detected (37). In the current study, CP-pDNA nanoparticles showed significantly lower cytotoxicity than PEI-pDNA polyplexes (Table S2), providing a desired balance of cytotoxicity and transfection efficiency. Compared with that of PEI-pDNA polyplexes in our previous study (19), the sustained release of CP-pDNA nanoparticles caused much lower cytotoxicity (Fig. 3a) and weaker inflammation reactions in subcutaneous tissues (Fig. 6a). Therefore, the use of CP-pDNA nanoparticles should provide clinical relevance for angiogenic gene delivery, along with the infusibility or injectability of electrosprayed microparticles into ischemic tissues or tissue engineering scaffolds. In addition, the incubation of PEG with 2 kDa into the microparticle matrices achieved a sustained release for 4 weeks, which was in accordance with the duration for the formation of mature blood vessel (4). The gradual release of CP-pDNA

nanoparticles resulted in strong protein expression (Fig. 4) and ECM secretion (Fig. 5) during 7 days of incubation, and enhanced the generation of blood vessels after subcutaneous infusion (Figs. 7 and 8). Therefore, the sustained release of pDNA ensured a long-term availability of signals at effective levels within the local tissue microenvironment for therapeutic vascularization and regeneration of functional tissues.

Angiogenesis involves a multi-step process, and multiple factors are usually required to increase the efficacy of angiogenesis. As a specific mitosis original of vascular ECs, VEGF can stimulate their proliferation, morphogenesis and differentiation, inhibit the apoptosis and strengthen the permeability of blood vessel (38). It is also quite clear that the application of only VEGF leads to the formation of immature and leaky vessels that cause diseases (39). bFGF, another important growth factor, not only cause the proliferation, morphogenesis and differentiation of many types of cells, but also can facilitate the recruitment of SMCs (40). The present study initially examined the efficacy of electrosprayed microparticles with the loading of both pVEGF and pbFGF to promote the cell function and tissue regeneration. The collagen secretion by ECs and α -SMA by SMCs after incubation with *Pv + b* were higher than those with *Pv* and *Pb* (Fig. 5). The subcutaneous infusion of *Pv-b* microparticles led to significantly higher densities of blood vessels and mature vessels than *Pv* and *Pb* microparticles (Figs. 7 and 8). It should be noted that the

sustained and localized co-delivery of pbFGF and pVEGF accelerated the maturation process of blood vessels. The amount of mature blood vessels after 2 weeks of administration of Pv-b microparticles was significantly higher those of Pv and Pb microparticles after 4 weeks of administration (Fig. 8). The above results indicated that a multiple delivery of pbFGF and pVEGF from electrosprayed microparticles is efficient to promote the formation of vascular network and induce the rapid generation of mature blood vessels.

CONCLUSIONS

The integration of pDNA condensation and electrospraying technologies was evaluated to promote the regeneration of blood vessels. Compared with commonly used pDNA polyplexes, CP-pDNA nanoparticles induced significantly lower cytotoxicity and few inflammation reactions after administration into animals. The sustained release of CP-pDNA nanoparticles led to incremental transfection efficiencies and strong ECM secretion of both ECs and SMCs. Compared with Pv and Pb microparticles, the multiple delivery of pbFGF and pVEGF promoted the cell proliferation and ECM secretion, resulted in significantly higher densities of blood vessels, and induced the rapid generation of mature blood vessels. The results suggested that electrosprayed microparticles with CP-pDNA nanoparticles encapsulated provided a clinically applicable and efficient method to promote the formation of vascular networks after injection to ischemic sites or entrapment into tissue engineering scaffolds.

ACKNOWLEDGMENTS AND DISCLOSURES

This work was supported by National Natural Science Foundation of China (51073130 and 21274117), Specialized Research Fund for the Doctoral Program of Higher Education (20120184110004), and Scientific and Technical Supporting Programs of Sichuan Province (2013SZ0084).

REFERENCES

- Phelps EA, Garcia AJ. Update on therapeutic vascularization strategies. *Regen Med*. 2009;4:65–80.
- Presta M, Dell'Era P, Mitola S, Moroni E, Ronca R, Rusnati M. Fibroblast growth factor/fibroblast growth factor receptor system in angiogenesis. *Cytokine Growth Factor Rev*. 2005;16:159–78.
- Carmeliet P, Baes M. Metabolism and therapeutic angiogenesis. *N Engl J Med*. 2008;23:2511–2.
- Formiga FR, Pelacho B, Garbayo E, Abizanda G, Gavira JJ, Simon-Yarza T, *et al*. Sustained release of VEGF through PLGA microparticles improves vasculogenesis and tissue remodeling in an acute myocardial ischemia—reperfusion model. *J Control Release*. 2010;147:30–7.
- Fu K, Klivanov AM, Langer R. Protein stability in controlled release systems. *Nat Biotechnol*. 2000;18:24–5.
- Jang JH, Rives CB, Shea LD. Plasmid delivery in vivo from: transgene expression and cellular transfection. *Mol Ther*. 2005;12:475–83.
- Guo R, Xu SJ, Ma L, Huang AB, Gao CY. The healing of full-thickness burns treated by using plasmid DNA encoding VEGF-165 activated collagen-chitosan dermal equivalents. *Biomaterials*. 2011;32:1019–31.
- Neumann S, Kovtun A, Dietzel ID, Epple M, Heumann R. The use of size-defined DNA-functionalized calcium phosphate nanoparticles to minimise intracellular calcium disturbance during transfection. *Biomaterials*. 2009;30:6794–802.
- Patil SD, Rhodes DG, Burgess DJ. DNA-based therapeutics and DNA delivery systems: a comprehensive review. *AAPS J*. 2005;7: E61–77.
- Truong-Le VL, Walsh SM, Schwabert E, Mao HQ, Guggino WB, August JT, *et al*. Gene transfer by DNA-gelatin nanospheres. *Arch Biochem Biophys*. 1999;361:47–56.
- Zhang MZ, Kataok K. Nano-structured composites based on calcium phosphate for cellular delivery of therapeutic and diagnostic agents. *Nano Today*. 2009;4:508–17.
- Stubbs M, McSheehy PMJ, Griffiths JR, Bashford CL. Causes and consequences of tumour acidity and implications for treatment. *Mol Med Today*. 2000;6:15–9.
- Curtin CM, Cunniffe GM, Lyons FG, Bessho K, Dickson GR, Duffy GP, *et al*. Innovative collagen nano-hydroxyapatite scaffolds offer a highly efficient non-viral gene delivery platform for stem cell-mediated bone formation. *Adv Mater*. 2012;24:749–54.
- Zhang S, Li J, Lykotrafitis G, Bao G, Suresh S. Size-dependent endocytosis of nanoparticles. *Adv Mater*. 2009;21:419–24.
- Kesisoglou F, Panmai S, Wu Y. Nanosizing—oral formulation development and biopharmaceutical evaluation. *Adv Drug Deliv Rev*. 2007;59:631–44.
- Enayati M, Chang MW, Bragman F, Edirisinghe M, Stride E. Electrohydrodynamic preparation of particles, capsules and bubbles for biomedical engineering applications. *Colloids Surf A*. 2011;382: 54–64.
- Wu YQ, Clark RL. Controllable porous polymer particles generated by electrospraying. *J Colloid Interf Sci*. 2007;10:529–35.
- Xie JW, Marijnissen JCM, Wang CH. Microparticles developed by electrohydrodynamic atomization for the local delivery of anticancer drug to treat C6 glioma in vitro. *Biomaterials*. 2006;27:3321–32.
- He SH, Xia T, Wang H, Wei L, Luo XM, Li XH. Multiple releases of polyplexes of plasmids VEGF and bFGF from electrosprayed fibrous scaffolds towards regeneration of mature blood vessels. *Acta Biomater*. 2012;8:2659–69.
- Deng X, Li X, Huang Z, Jia W, Zhang Y. Optimization of preparative parameters for poly-DL-lactide-poly(ethylene glycol) microspheres with entrapped *Vibrio cholera* antigens. *J Control Release*. 1999;58:123–31.
- Morgan TT, Muddana HS, Altinoglu EI, Rouse SM, Tabakovic A, Tabouillot T, *et al*. Encapsulation of organic molecules in calcium phosphate nanocomposite particles for intracellular imaging and drug delivery. *Nano Lett*. 2008;8:4108–15.
- Wu YQ, Liao IC, Kennedy SJ, Du JZ, Wang J, Leong KW, *et al*. Electrosprayed core-shell microspheres for protein delivery. *Chem Commun*. 2010;46:4743–5.
- Yang Y, Li XH, Cheng L, He SH, Zou J, Chen F, *et al*. Core-sheath-structured fibers with pDNA polyplex loadings for optimal release profile and transfection efficiency as potential tissue engineering scaffolds. *Acta Biomater*. 2011;7:2533–43.
- Becker TA, Kipke DR, Brandon T. Calcium alginate gel: a biocompatible and mechanically stable polymer for endovascular embolization. *J Biomed Mater Res*. 2001;54:76–86.

25. Okazaki M, Yoshida Y, Yamaguchi S, Kaneno M, Elliott JC. Affinity binding phenomena of DNA onto apatite crystals. *Biomaterials*. 2001;22:2459–64.
26. Dorozhkin SV, Epple M. Biological and medical significance of calcium phosphates. *Angew Chem Int Ed*. 2002;41:3130–46.
27. Elliott JC. Structure and chemistry of the apatites and other calcium orthophosphates. Amsterdam: Elsevier; 1994. p. 1–12.
28. Chakraborty S, Liao IC, Adler A, Leong KW. Electrohydrodynamics: a facile technique to fabricate drug delivery systems. *Adv Drug Deliv Rev*. 2009;61:1043–54.
29. Kelleher CM, McLean SE, Mechem RP. Vascular extracellular matrix and aortic development. *Curr Top Dev Biol*. 2004;62:153–88.
30. Adelow C, Segura T, Hubbell JA, Frey P. The effect of enzymatically degradable poly(ethylene glycol) hydrogels on smooth muscle cell phenotype. *Biomaterials*. 2008;29:314–26.
31. Fujita M, Ishihara M, Simizu M, Obara K, Ishizuka T, Saito Y. Vascularization in vivo caused by the controlled release of fibroblast growth factor-2 from an injectable chitosan/non-anticoagulant heparin hydrogel. *Biomaterials*. 2004;25:699–706.
32. Wei L, Lin J, Cai C, Fang Z, Fu W. Drug-carrier/hydrogel scaffold for controlled growth of cells. *Eur J Pharm Biopharm*. 2011;78:346–54.
33. Taylor AP, Rodriguez M, Adams K, Goldenberg DM, Blumenthal RD. Altered tumor vessel maturation and proliferation in placenta growth factor producing tumor: potential relationship to post-therapy tumor angiogenesis and recurrence. *Int J Cancer*. 2003;105:158–64.
34. Yancopoulos GD, Davis S, Gale NW, Rudge JS, Wiegand SJ, Holash J. Vascular-specific growth factors and blood vessel formation. *Nature*. 2000;407:242–8.
35. Nillesen STM, Geutjes PJ, Wiismans R, Schalkwijk J, Daamen WF, van Kuppevelt TH. Increased angiogenesis and blood vessel maturation in acellular collagen—heparin scaffolds containing both FGF2 and VEGF. *Biomaterials*. 2007;28:1123–31.
36. Folkman J. Angiogenesis in cancer, vascular, rheumatoid and other disease. *Nat Med*. 1995;1:27–31.
37. Ye L, Zhang W, Su LP. Nanoparticle based delivery of hypoxia-regulated VEGF transgene system combined with myoblast engraftment for myocardial repair. *Biomaterials*. 2011;32:2424–31.
38. Hendel RC, Henry TD, Rocha-Singh K, Isner JM, Kereiakes DJ, Giordano FJ, et al. Effect of intracoronary recombinant human vascular endothelial growth factor on myocardial perfusion: evidence for a dose-dependent effect. *Circulation*. 2000;101:118–21.
39. Zacchigna S, Tasciotti E, Kusmic C, Arsic N, Sorace O, Marini C, et al. In vivo imaging shows abnormal function of vascular endothelial growthfactor-induced vasculature. *Hum Gene Ther*. 2007;18:515–24.
40. Klagsbrun M. The fibroblast growth factor family: structural and biological properties. *Progr Growth Factor Res*. 1989;1:207–35.